Effect of annealing conditions on the superconducting properties of nano-sized metallic Au-added $Bi_{1.8}Sr_2Au_{0.2}Ca_{1.1}Cu_{2.1}O_y$ (Bi-2212) ceramics

Berdan Özkurt[1]

Abstract

In this study, the effects of annealing process on the phase formation and electrical and magnetic properties of nano-sized metallic Au-added Bi-2212 ceramics have been investigated. The $Bi_{1.8}Sr_2Au_{0.2}Ca_{1.1}Cu_{2.1}O_y$ including $x = 0.2$ Au content as starting composition was chosen due to the improved transport properties in the Bi-2212 system, as known in the literature. The samples for the post-annealing technique were exposed at different dwell times (10 m, 30 m, 1 h, and 2.5 h) at a fixed temperature of 870 °C after the application of normal heat treatment of 850 °C for 120 h. The XRD diagrams clearly indicate that a significant part of the phases in all the samples belongs to Bi-2212 phase. SEM results show that all the samples have randomly oriented grain forms as the main characteristic of applied solid-state method. In all cases, the post-annealed samples showed better superconducting properties of Bi-2212 phase, indicating that the increases in the dwell time positively affect its granular polycrystalline character such as inter-connectivity of the grains, the nucleation, and growth of the Bi-2212 phase. Moreover, the sample with dwell time of 2.5 h at 870 °C reveals significant enhancement in the *M–H* loops compared to the sample with less dwell time, despite the fact that the Bi-2212 phase can easily decompose into secondary phases such as Cu-free and Bi-free due to thermodynamic instabilities of Bi-2212 at temperatures above 860 °C. Finally, the intragranular critical current density values (J_c) have been obtained by using the data from M-H measurements according to the critical Bean model. It has been found that the J_c value (16.5×10^4 A/cm^2 in 0.15 T at 15 K) of the sample in the dwell time of 2.5 h at 870 °C is higher than that of the sample (13.4×10^4 A/cm^2 in 0.15 T at 10 K) with the same starting composition reported in the literature.

1 Introduction

Bi–Sr–Ca–Cu–O (BSCCO) system including three different superconducting phases of Bi-2201, Bi-2212, and Bi-2223 with the general formula $Bi_2Sr_2Ca_{n-1}Cu_nO_{4+2n}$ ($n = 1, 2, 3$) has become one of the most promising materials in realizing technological applications of high-temperature superconductors [1–8]. Among a large number of existing high-T_c materials, after three decades of their intensive investigation all over the world, only two systems are selected for technical application in electrical engineering for cable production and for superconducting magnet design: Bismuth-based and 123-YBaCuO materials [9]. Nonetheless, there are still many

problems that need to be solved such as low critical current density at high magnetic fields, the weak links between the grains, and the lack of effective pinning centers in the BSCCO system.

Despite all these problems, there are many studies in the literature, showing that the electrical and magnetic properties of the BSCCO ceramics can be enhanced by the substitution or the addition of different elements at the optimal contents such as Pb, Li, K, Er, B, Nb, Cd, Sn, Ag, and so on. [10–26]. Moreover, the specific techniques such as laser floating zone (LFZ) and the electrically assisted laser floating zone (EALFZ) ensuring better grain orientations and stronger grain connections also are quite useful to obtain high critical current density (J_c) as well as the formation of high-T_c phases in the BSCCO system [27–31]. It is well known that the width of the hysteresis loops (*M-H*) in type II superconductors, which is proportional to the J_c values, strongly depends on the changes in the shape, arrangement, and size of the grains. Especially,

✉ Berdan Özkurt
berdanozkurt@tarsus.edu.tr

1   Department of Natural and Mathematical Sciences, Faculty of Engineering, Tarsus University, 33400 Tarsus, Turkey

the formation of large grain sizes together with a smooth grain alignment can provide high current density [32]. One of the most effective methods to achieve the desired large grain sizes in the BSCCO system is the optimization of the calcination and sintering stages [33].

In many works, it has been reported that J_c values of the BSCCO ceramics can be significantly increased by the post-annealing technique which is defined as extra heat treatment after application of the standard temperature periods required for crystallization of ceramic materials [30, 34–39]. The main reason for the formation of higher J_c values in the ceramic superconductors produced by that procedure is usually connected with the increasing number of effective pinning centers ensured by the controlled decomposition of the superconducting phase or the formation of more granular morphology with larger grain sizes as a consequence of the applied long sintering conditions at high temperatures. However, these processes may also lead to the formation of different impurity phases that cause important deteriorations in the superconducting properties of the BSCCO system due to the excess of any of the oxide constituents in the system Bi–Pb–Sr–Ca–Cu–O (BPSCCO). Thus, it is very important to control the parameters such as temperature and time to be applied for extra thermal processes, which are responsible for supporting the regular crystallization of the desired phases in a high density and the formation of large grains with low porosity, ensuring high degrees of texture.

In fact, the main existing problem of high-T_c superconducting materials is the rapid decrease of critical current in external magnetic fields. One of the main methods to improve superconducting properties of those materials is introduction of artificial pinning centers for increasing of the pinning force and as a result, there is an increase the activation energy of magnetic fluxe motion and critical current density in strong magnetic fields, respectively. Generally, it is observed from the literature that there are many methods such as the introduction of non-superconducting nanoparticles, substitution of Cu by some other cations, creation of radiation defects using ion implantation, and neutron or electron irradiation in the generation of artificial pinning centers [40]. Therefore, the effects of partial element substitutions on their J_c performance in high-temperature superconductors as well as magnetic nanoparticles serving as very effective pinning centers were studied by many research groups [41–46].

Moreover, previous works have demonstrated that the substitution or addition of metallic elements such as Ag and nano-sized Au into BSCCO system also affects its mechanical properties as well as its T_c and J_c values positively [6, 34, 47–52]. It is obvious that the $Bi_{1.8}Sr_2Au_{0.2}Ca_{1.1}Cu_{2.1}O_y$ including nano-sized metallic Au at $x=0.02$ content also

ensures better intergranular conductivity besides the formation of the high amounts of Bi-2212 phase, showing that it can be selected as initial composition.

The post-annealing process for this work has been applied to the nano-sized metallic Au (15 nm)-added $Bi_{1.8}Sr_2Au_{0.2}Ca_{1.1}Cu_{2.1}O_y$ composition following the application of classical preparation conditions as reported previously [50]. In the process, with the temperature kept constant at 870 °C, the annealing times of the samples in the post-annealing procedure have been selected as 10 min, 30 min, 1 h, and 2.5 h, respectively.

The present paper proposes a novel method consisting in the following combination:

– partial substitution of cations in Bi-based 2212 material by Au, and
– a special program of annealing treatment.

Thus, a noticeable improvement of the polycrystalline samples' morphology and quality can be expected with improved intergrain connection as based on better connectivity between superconducting grains, which leads to improvement of the superconducting properties of prepared samples.

The results obtained in this study reveal that in order to obtain enhanced superconducting properties of the Bi-2212 phase in the $Bi_{1.8}Sr_2Au_{0.2}Ca_{1.1}Cu_{2.1}O_y$ composition, it is necessary to perform the post-annealing process with relatively small increments of time and temperature gradients on the nominal crystallization time and temperature of the Bi-2212 phase.

2 Experimental details

Polycrystalline samples of $Bi_{1.8}Sr_2Au_{0.2}Ca_{1.1}Cu_{2.1}O_y$ as a starting composition were prepared by the standard solid-state reaction method. High-purity powders of commercial Bi_2O_3 (Panreac, 98+ %), $SrCO_3$ (Panreac, 98+ %), $CaCO_3$ (Panreac, 98.5+ %), CuO (Panreac, 97+ %), and metallic Au (Nanografi Co. Ltd., 15 nm, 99.9+ %) were used for the preparation of ceramics. They were weighed in the appropriate proportions and were mixed and milled. After the milling process, the homogenous mixture of powders was pressed into pellets of 1.3 cm diameter by applying a 375 MPa pressure and calcined at 750 °C for 12 h. The calcined pellets were reground, repressed, and recalcined twice at 820 °C for 24 h to start the formation of the superconducting phase. The experimental processes of the previous article, which is described in detail [50], were exactly applied during the preparation of samples in this work to better observe the effect of post-annealing on the samples of $Bi_2Sr_2Au_{0.2}Ca_1Cu_{1.8}O_y$ (Bi-2212). Finally, precursor

materials were ground and repressed, and annealed at 850 °C for 120 h in order to reach a large amount of pure Bi-2212.

After their final heat treatments, the annealing process of the samples is carried out using different dwell times (10 m, 30 m, 1 h, and 2.5 h) at a constant temperature of 870 °C. Taking into account the dwell times at a constant temperature of 870 °C, the samples will be here after denoted as A, B, C, and D, respectively. Heating schedule of post-annealing procedure clearly is shown in Fig. 1.

Resistivity and magnetic measurements were carried out on samples using Cryogenic Limited PPMS (from 5 to 300 K) which can reach the cryogenic temperatures about to 2 K in a closed-loop He system. X-ray powder diffraction analyses to determine the phases present in the samples were performed by using a Rigaku Ultima IV X-ray diffractometer with a constant scan rate (2 degree/minute) in the range of $2\theta = 3°–60°$. Lattice parameters have been automatically calculated by the PDXL software version 1.6.0.1 with the ICDD version 6.0 database. The surface morphologies of the samples were studied by using a Zeiss LS-10 Life Science scanning electron microscopy (SEM).

3 Results and discussion

3.1 XRD studies

Powder XRD patterns of all the samples are shown in Fig. 2. All main peaks of the annealed samples are indexed as Bi-2212 phase, indicating that the samples were successfully synthesized without disturbing the thermal stability of the Bi-2212 phase. When compared with the intensities and positions of the peaks belonging Bi-2212 phase in all the samples, they did not show significant changes. However, some minor impurity phases such as $Bi_4Sr_4CaCu_3O_4$ and Bi_2CaO_4 were also detected for all the samples in the powder XRD patterns of the samples. Note that the formation of secondary phases in the ceramic superconductors, which mean the important changes in the peak positions of main

Bi-2212 phase, is generally associated with a two-step drop in the resistive transitions. Therefore, the impurity phases detected in this work can cause a wide range in the transitions between the normal and superconducting states. On the other hand, it is obvious that the intensity and positions of peaks of those impurity phases are almost stable. This means that the selected post–annealing conditions in this work do not cause significant damages on their basic magnetic properties including the characteristic diamagnetic behavior due to the formation of high amounts of Bi-2212 phase in the samples even if the annealing conditions significantly change the growth of the grains and the kinetics of formation of phases in the BSSCO system [33]. On the other hand, unit cell parameters of all the samples are given in Table 1. There is a systematic increase in the lattice parameter c of samples with increasing of dwell time in their post-annealing process. In general, the Bi-2212 phase can easily decompose into the secondary phases at the applied temperatures above or below its melting point due to degradation of the chemical stability of the Bi-2212 phase. In this case, it is also obvious that there will be important shifts in the peak position of the Bi-2212 phase as well as new peaks observing in XRD due to the formation of new impurity phases in different types. In contrast, the longitudinal values of the c-lattice parameters of the Bi-2212 phase in this work gradually increase with increasing post-annealing periods and the highest value is obtained in sample D of 30.807 values, as seen in Table 1. This means that the chemical composition of the Bi-2212 phase is protected during applied annealing steps. The interaction between the (BiO) double layers is responsible for the values of the c-axis, showing the axial height of the unit cell of BSCCO. The changing amount of oxygen in the BiO layers affects the interaction between them and causes the c unit parameter to change.

Thus, systematic increase in c-lattice parameter observed in Table 1 clearly shows that the selected time and temperature for post-annealing conditions in the $Bi_{1.8}Sr_2Au_{0.2}Ca_{1.1}Cu_{2.1}O_y$ composition positively contribute to the adjustment of the amount of oxygen as well as the formation kinetics and stabilization of desired Bi-2212 phases.
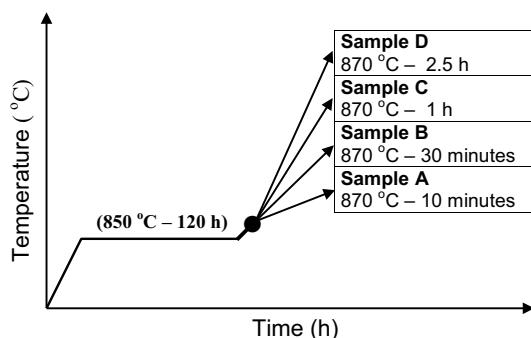
3.2 SEM studies

Figure 3 shows the characteristic SEM micrographs of the annealed samples for different dwell times at a constant temperature of 870 °C. In general, the thermal stability range of Bi-2212 phase is much higher compared with other phases of the BSCCO ceramics, implying that the grains with large size and high density in the formation of Bi-2212 phases can be obtained when long heat treatments are applied in composition Bi-2212. It is obvious from Fig. 3 that all the samples have the granular morphology at similar grain orientations. As seen from
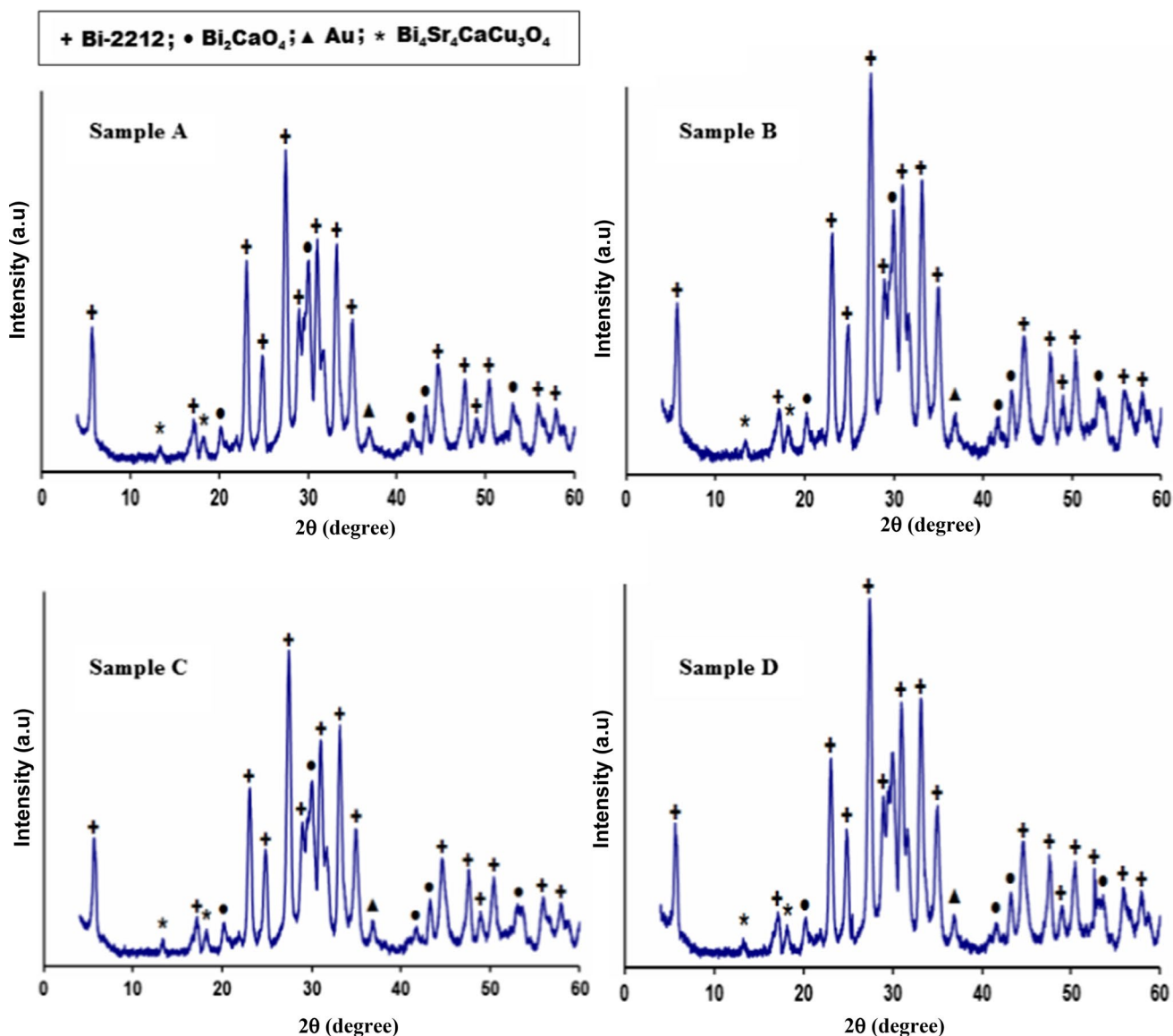

Fig. 1 Heating schedule of post-annealing procedure

Fig. 2 XRD patterns of the A, B, C, and D samples. The symbols indicate the different phases: + Bi-2212; ● Bi_2CaO_4; ▲ Au; * $Bi_4Sr_4CaCu_3O_4$

Table 1 Lattice parameters and resistivity measurement results for the samples

Samples	a (Å)	b (Å)	c (Å)	T_c^{onset} (K)	T_c^{offset} (K)	R (mΩ cm) at 150 K
A	3.8134	3.8134	30.669	78.2	58.1	1.29
B	3.8224	3.8224	30.705	76.4	59.9	0.903
C	3.8112	3.8112	30.713	77.3	59.4	0.95
D	5.4043	5.4043	30.807	79.5	60.06	1.06

the XRD graphs of the samples, the peak intensities of Bi-2212 phase at different annealing times applied do not change significantly. On the other hand, the relationship between grain sizes and peak intensities of the phases observed in the XRD patterns may be calculated using the Scherrer–Warren equation [53–55]. Thus, it is quite normal to observe similar grain structures, when the unchanged intensity of XRD peaks obtained in this study is taken into account. However, the change of basic factors such as different grain boundary densities, the grain
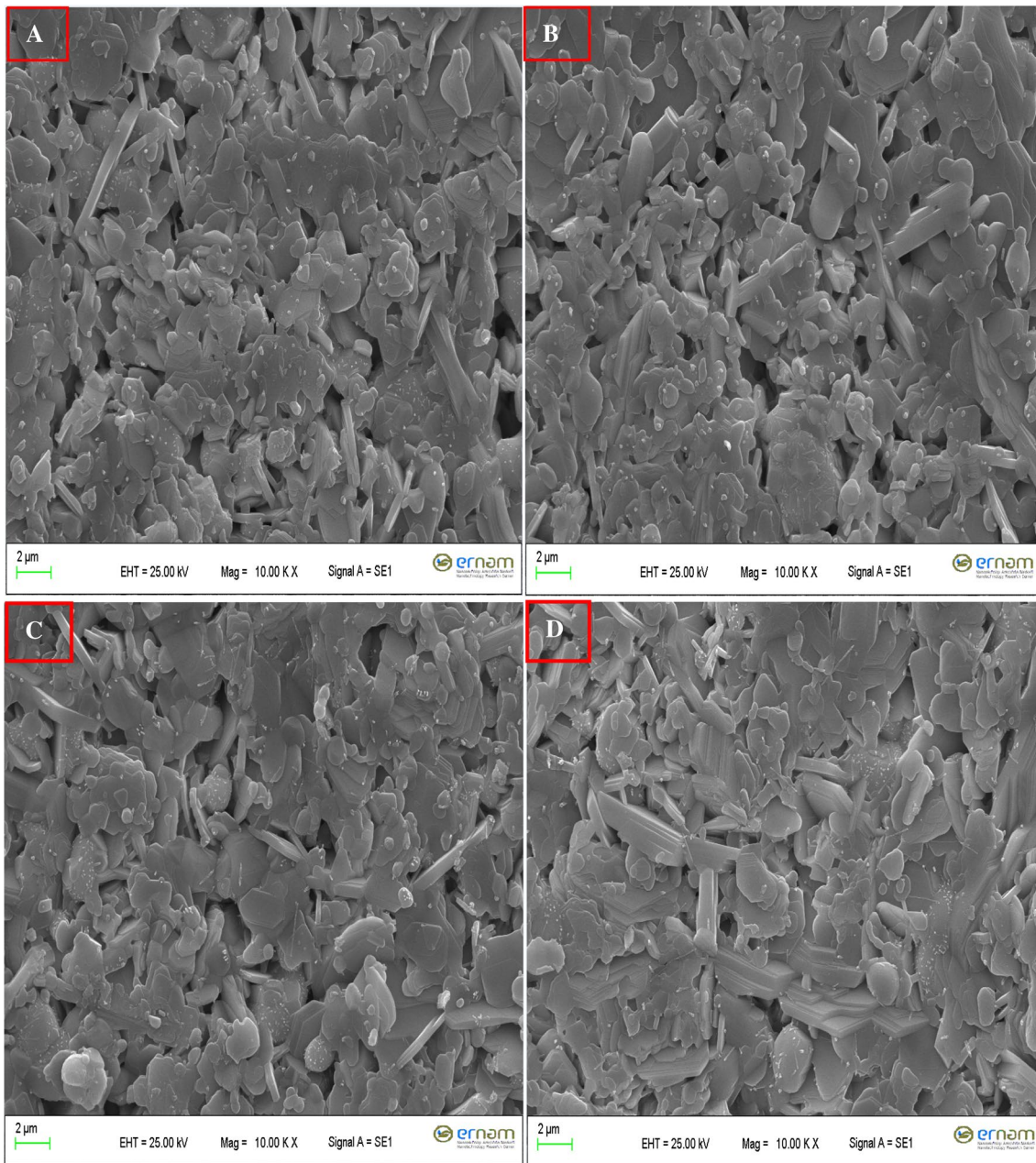
Fig. 3 SEM micrographs obtained in the surfaces of **a** A; **b** B; **c** C; and **d** D samples

boundary width and the presence of voids at different contents can also cause significant differences in J_c values of the samples. Moreover, the random distribution of grains with a plate-like morphology is clearly seen in all the samples due to the solid-state reaction method used for the preparation of the samples in this work. This also explains the reason for some voids observed in the SEM pictures of the samples. In general, the high volatility of the Bi element as a result of long heat treatments used for the post-annealing process can cause the partially melted region, limiting the improvement of the grain connectivity

and the stability of the Bi-2212 phase [56]. On the other hand, the colors of the grains observed in SEM images provide important information about the phases formed. In the literature, it is well known that the gray contrast is generally associated with the Bi-2212 phases while the black and dark gray ones reflect CaO and (Sr, Ca)–Cu–O phases, respectively [29, 57]. It can be observed from SEM images for all samples that they have the formation of grains with gray contrast in high amounts, reflecting the presence of Bi-2212 phases. Thus, it can be said from the size and color contrasts of the grains that the different dwell times

performed at a constant temperature of 870 °C support the kinetics of formation of the Bi-2212 phase in agreement with the XRD results.

3.3 Resistivity measurements

Figure 4 shows the resistive transition behavior of all the samples. The change in resistivity observed in the transition range from the normal to the superconducting state in this work is nearly the same (superconducting transition width ΔT_c), suggesting the formation of similar phases in
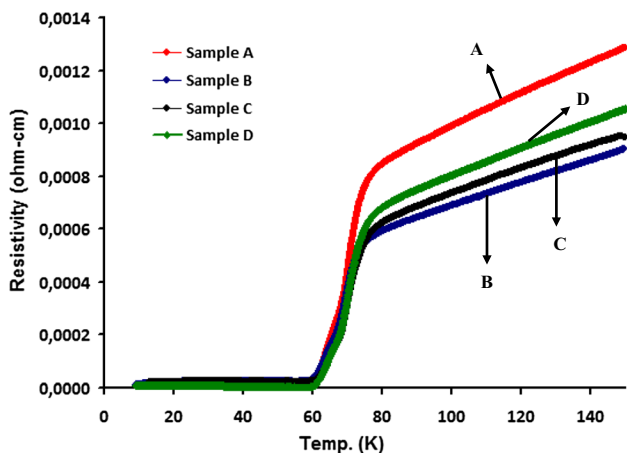
Fig. 4 Electrical resistivity as a function of temperature curves for all the samples

the samples. Moreover, all the samples with high values of T_c (onset) over 76 K exhibit a one-step transition behavior, even if the transition from normal to superconducting state is wide ($\Delta T \approx 20$ K) due to the effect of impurity phases. Generally, T_c (onset) values in the high-T_c superconductors significantly depend on the formation of the Bi-2212 phase. In accordance with the XRD and SEM results, T_c (onset) values in all the samples remain close to the ideal values of the Bi-2212 phase. This means that the applied procedure does not have a negative effect on the formation of the Bi-2212 phase, showing that the electrical properties of Bi-2212 phase can be improved with extra time and temperature adjustments.

On the other hand, another of the most important factors for improving transition temperatures is the creation of more holes in the CuO_2 sheet [58].

The results clearly show that the sample D annealed for 2.5 h at 870 °C has the highest T_c (onset) and T_c (offset) values (see Table 1). These trends can be notoriously explained by high phase purity and a better crystallization reflecting more granular structure. By maintaining the annealing temperature of 870 °C and increasing further the post-annealing time to 2.5 h, more charge balance in the CuO_2 layers can occur in sample D.

3.4 DC magnetic properties

Figure 5 shows the magnetic hysteresis cycles (*M–H*) presented between applied fields of ± 2 T at both 5 and 15 K
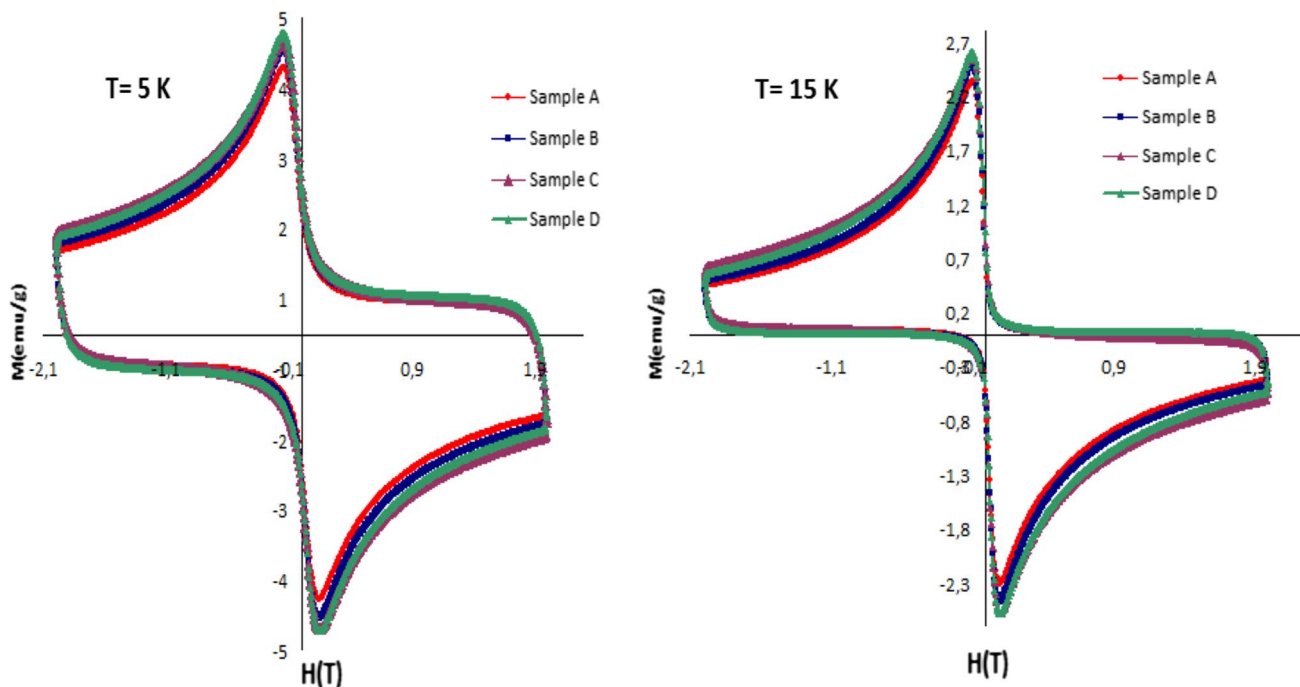
Fig. 5 Magnetization hysteresis curves for all samples measured at 5 K and 15 K for ± 2 T externally applied magnetic field

for all the samples, respectively. It is obvious from the XRD and SEM results that the Bi-2212 superconducting phase is dominant in all the samples. As can be seen from the *M–H* results, all samples exhibit diamagnetic behavior in a very similar way due to the characteristic magnetic properties of the predominant Bi-2212 phases. On the other hand, it is well known that the area of hysteresis loops in ceramic superconductors is higher when the orientation of grains, together with strong-linked grain boundaries, is regular. Also, the amount of impurity phases and the degree of connectivity between grains significantly affect the areas and shape of the hysteresis loops. Although relatively short annealing times at higher temperatures than the characteristic crystallization temperature of Bi-2212 ceramics (> 850–860 °C) are applied to the samples, a steady increase in the areas of *M–H* loops has been observed with increasing dwell times in this work. This means that the above-mentioned conditions related to the orientation and the connection of the grains positively improve with the post-annealing process applied.

The J_c values of the samples were calculated for the two different temperatures, 5 and 15 K, using Bean's model [59]:

$$J_C = F\frac{\Delta M}{d},$$

where J_C is the critical current density in ampéres per square centimeter of a sample, $\Delta M = M_+ - M_-$ sample magnetization at increasing (+) and decreasing (−) external magnetic field, measured in electromagnetic units per cubic centimeter, d is the diameter of a cylindrical sample (pellet) measured in cm, and F is the demagnetizing factor, which depends on the sample geometry. For this pellet $F = 30$.

In Fig. 6, the magnetic field variation of the J_c for all samples has been plotted. In previous work, the highest J_c value for $Bi_{1.8}Sr_2Au_{0.2}Ca_{1.1}Cu_{2.1}O_y$ sample with $x = 0.2$ Au additions has been obtained as 13.42×10^4 A/cm² in 0.15 T at 10 K. In the present study, the highest J_c in the sample D, which is exposed to the extra annealing period of 2.5 h

at 870 °C on the $Bi_{1.8}Sr_2Au_{0.2}Ca_{1.1}Cu_{2.1}O_y$ composition of the starting material, reached 16.58×10^4 A/cm² in 0.15 T at 15 K. As can be seen form Fig. 6, all the J_c values at both 5 and 15 K are found to increase with increase in dwell times, when the applied magnetic field ranges from 0 to 2 T. It is well known that the J_c values in high-temperature superconductors decrease rapidly with increasing field at high temperatures. Moreover, the intrinsic intragrain characteristics as well as the formation and stabilization of the desired phases play an important role in the enhancement of the critical current density, especially at high temperatures. However, the factors such as the intergrain couplings, the angle of the grain boundaries, and the orientation of the grains significantly affect the values of J_c at relatively lower temperatures (< 30 K). Especially, the extra heat treatments applied at optimal values in the BSCCO system positively affect the microstructure of grains on the nanometer scale [60]. Thus, the increases in J_c values observed at low temperatures in this study depend on positively adjusting the weak-link behavior of grain boundaries and the irregularities in grain shapes with the applied annealing procedures, ensuring a lower possible range of porosity.

4 Conclusions

In this study, the effect of annealing time (10 m, 30 m, 1 h, and 2.5 h) at 870 °C on the physical and superconducting properties of the Bi-2212 phase in the $Bi_{1.8}Sr_2Au_{0.2}Ca_{1.1}Cu_{2.1}O_y$ starting composition is analyzed by means of the XRD, SEM, DC resistivity, magnetic hysteresis loops (*M–H*), and the intragranular J_c values calculated by using their *M–H* data. The formation of plate-like grains, which are typically observed in SEM images of the Bi-2212 surface, was confirmed for all the samples exposed to different dwell times in the case of annealing at 870 °C for 2.5 h after keeping at 850 °C for 120 h.

Fig. 6 Calculated critical current densities for all the samples at 5 K and 15 K as a function of applied field
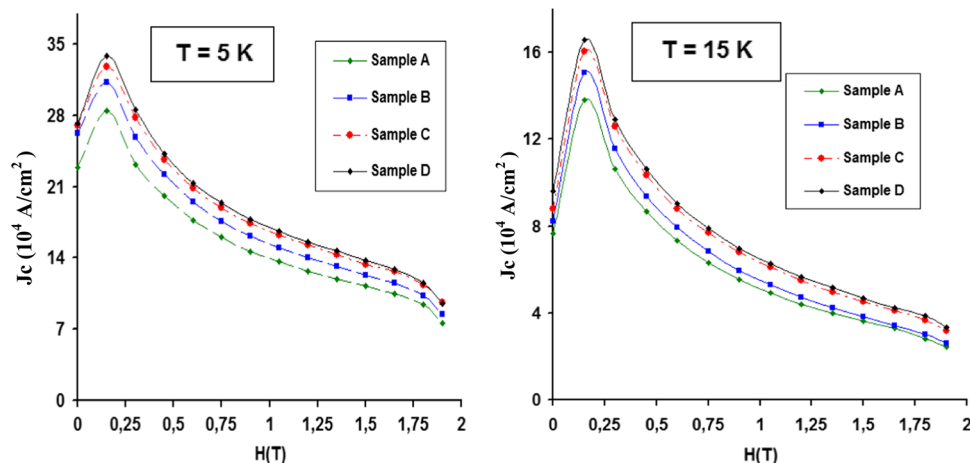
In addition, no melt parts were observed isolated locally in the SEM images for all the samples, meaning that the applied heat treatments positively affect the crystallization temperature of the Bi-2212 phase probably due to the amount of nano-sized metallic Au expected to be present in the starting composition. Also, it is observed from Table 1 that both T_c (onset) and T_c (offset) temperatures of superconducting transition are the highest for the sample D containing the longest dwell time of 2.5 h at 870 °C.

These results clearly suggest that the physical and magnetic properties of Bi-2212 phase with a nominal composition of $Bi_{1.8}Sr_2Au_{0.2}Ca_{1.1}Cu_{2.1}O_y$ can be optimized by post-annealing performed at 870 °C, ensuring better connectivity between superconducting grains and a high rate of formation of the Bi-2212 phase.

References

1. H. Maeda, Y. Tanaka, M. Fukutomi, T. Asano, Jpn. J. Appl. Phys. **27**, L209–L210 (1988)
2. M. Takano, J. Takada, K. Oda, H. Kitaguchi, Y. Miura, Y. Ikeda, Y. Tomii, H. Mazaki, Japan. J. Appl. Phys. Lett. **45**, 27–L1041 (1988)
3. C. Michel, M. Hervieu, M.M. Borel, A. Grandin, F. Deslandes, J. Provost, B. Raveau, Z. Phys. B **68**, 421–423 (1987)
4. H.G. von Schnering, L. Walz, M. Schwarz, W. Becker, M. Hartweg, T. Popp, B. Hettich, P. Muller, G. Kampf, Angew. Chem. Int. Ed. Engl. **27**, 574–576 (1988)
5. G. Blatter, M.V. Feigelman, V.B. Ceshkenbein, A.I. Larkin, V.M. Vinokur, Rev. Mod. Phys. **66**, 1125–1388 (1994)
6. G. Yıldırım, J. Alloys Compd. **699**, 247–255 (2017)
7. R. Heller, J.R. Hull, I.E.E.E. Trans, Appl. Supercond. **5**, 797–800 (1995)
8. D. Sharma, R. Kumar, V.P.S. Awana, Ceram. Int. **39**, 1143–1152 (2013)
9. D.S. Ginley, D.A. Cardwell (eds.), *Handbook of Superconducting Materials: Characterization, Applications and Cryogenics* (Institute of Physics, Philadelphia, 2003)
10. A.B. Kulakov, I.K. Bdikin, S.A. Zver'kov, G.A. Emel'chenko, G. Yang, J.S. Abell, Physica C **371**, 45–51 (2002)
11. O. Bilgili, Y. Selamet, K. Kocabaş, J. Supercond. Novel Magn. **21**, 439–449 (2008)
12. H. Sözeri, N. Ghazanfari, H. Özkan, A. Kılıç, Supercond. Sci. Technol. **20**, 522–528 (2007)
13. A. Sotelo, M. Mora, M.A. Madre, J.C. Diez, L.A. Angurel, G.F. de la Fuente, J. Eur. Ceram. Soc. **25**, 2947–2950 (2005)
14. L. Jiang, Y. Sun, X. Wan, K. Wang, G. Xu, X. Chen, K. Ruan, J. Du, Physica C **300**, 61–66 (1998)
15. S. Zhang, C. Li, Q. Hao, X. Ma, T. Lu, P. Zhang, Supercond. Sci. Technol. **28**, 045014 (2015)
16. N.G. Margiani, I.R. Metskhvarishvili, Z.A. Adamia, T.D. Medoidze, N.A. Papunashvili, D.I. Dzanashvili, M.I. Chubabria, J. Supercond. Novel Magn. **26**, 965–968 (2013)
17. M. Zargar Shoushtari, S.E. Mousavi Ghahfarokhi, J. Supercond. Novel Magn. **24**, 1505–1511 (2011)
18. A.I. Abou Aly, M.M.H. Abdel Gawad, R. Awad, I.G. Eldeen, J. Supercond. Novel Magn. **24**, 2077–2084 (2011)
19. G. Kırat, O. Kızılaslan, M.A. Aksan, Ceram. Int. **42**, 15072–15076 (2016)
20. M. Mora, A. Sotelo, H. Amaveda, M.A. Madre, J.C. Diez, L.A. Angurel, G.F. de la Fuente, Bol. Soc. Esp. Ceram. **44**, 199–203 (2005)
21. S. Şakiroğlu, K. Kocabaş, J. Supercond. Novel Magn. **24**, 1321–1325 (2011)
22. S.M. Khalil, J. Phys. Chem. Solids **62**, 457–466 (2001)
23. A. Sotelo, M.A. Madre, J.C. Diez, Sh Rasekh, L.A. Angurel, E. Martinez, Supercond. Sci. Technol. **22**, 034012 (2009)
24. M.A. Madre, H. Amaveda, M. Mora, A. Sotelo, L.A. Angurel, J.C. Diez, Bol. Soc. Esp. Ceram. **47**, 148–152 (2008)
25. Y.L. Chen, R. Stevens, J. Am. Ceram. Soc. **75**, 1150–1159 (1992)
26. R. Ramesh, G. Thomas, S. Green, C. Jiang, Y. Mei, M.L. Rudee, H.L. Luo, Phys. Rev. B **38**, 7070–7073 (1988)
27. B. Özçelik, B. Özkurt, M.E. Yakıncı, A. Sotelo, M.A. Madre, J. Supercond. Novel Magn. **26**, 873–878 (2013)
28. B. Özkurt, M.A. Madre, A. Sotelo, M.E. Yakıncı, B. Özçelik, J. Supercond. Novel Magn. **25**, 799–804 (2012)
29. B. Özkurt, M.A. Madre, A. Sotelo, M.E. Yakıncı, B. Özçelik, J.C. Diez, J. Supercond. Novel Magn. **26**, 1093–1098 (2013)
30. B. Özkurt, M.A. Madre, A. Sotelo, J.C. Diez, Phys. B **426**, 85–89 (2013)
31. F.M. Costa, Sh Rasekh, N.M. Ferreira, A. Sotelo, J.C. Diez, M.A. Madre, J. Supercond. Novel Magn. **26**, 943–946 (2013)
32. B. Zeimetz, S.X. Dou, H.K. Liu, Supercond. Sci. Technol. **11**, 1082–1086 (1998)
33. V. Garnier, I. Monot, G. Desgardin, Supercond. Sci. Technol. **13**, 602–611 (2000)
34. B. Özkurt, J. Supercond. Novel Magn. **31**, 2459–2464 (2018)
35. B. Özkurt, M.A. Madre, A. Sotelo, J.C. Diez, J. Supercond. Novel Magn. **26**, 3247–3252 (2013)
36. A. Sotelo, M.A. Madre, S. Rasekh, G. Constantinescu, M.A. Torres, J.C. Diez, J. Supercond. Novel Magn. **26**, 985–990 (2013)
37. G. Yildirim, A. Varilci, M. Akdogan, C. Terzioglu, J. Mater. Sci. Mater. Electron. **23**, 928–935 (2012)
38. M. Viret, J.F. Lawler, J.G. Lunney, Supercond. Sci. Technol. **6**, 490–496 (1993)
39. V. Garnier, R. Caillard, A. Sotelo, G. Desgardin, Physica C **319**, 197–208 (1999)
40. H. Maeda (ed.), *Bismuth-Based High-Temperature Superconductors* (CRC Press, Boca Raton, 1996)
41. A. Sidorenko, E.W. Scheidta, F. Haidera, M. Klemma, S. Horna, L. Konopkob, R. Tideckta, Phys. B **321**, 298–300 (2002)
42. E. Taylan Koparan, A. Surdu, A. Awawdeh, A. Sidorenko, E. Yanmaz, J. Supercond. Novel Magn. **25**, 1761–1767 (2012)
43. E. Taylan Koparan, A. Surdu, A. Sidorenko, E. Yanmaz, Physica C **473**, 1–5 (2012)
44. A.E. Surdu et al., Beilstein J. Nanotechnol. **2**, 809–813 (2011)
45. Z.Y. Jia, H. Tang, Z.Q. Yang, Y.T. Xing, Y.Z. Wang, G.W. Qiao, Physica C **337**, 130–132 (2000)
46. B. Zhao, W.H. Song, X.C. Wu, J.J. Du, Y.P. Sun, H.H. Wen, Z.X. Zhao, Physica C **361**, 283–291 (2001)
47. Y. Zalaoglu, G. Yildirim, J. Mater. Sci. Mater. Electron. **28**, 17693–17701 (2017)
48. N.K. Saritekin, M. Pakdil, E. Bekiroglu, G. Yildirim, J. Alloys Compd. **688**, 637–646 (2016)
49. Y. Zalaoglu, F. Karaboga, C. Terzioglu, G. Yildirim, Ceram. Int. **43**, 6836–6844 (2017)

50. U. Öztornacı, B. Özkurt, Ceram. Int. **43**, 4545–4550 (2017)
51. B. Özkurt, J. Mater. Sci. Mater. Electron. **30**, 14547–14553 (2019)
52. B. Özkurt, M.A. Madre, A. Sotelo, J.C. Diez, J. Mater. Sci. Mater. Electron. **24**, 3344–3351 (2013)
53. J. Economy, R. Anderson, Inorg. Chem. **5**, 989–992 (1966)
54. J. Jiang, Mater. Lett. **61**, 3239–3242 (2007)
55. F. Haque, K.S. Rahman, M. Akhtaruzzaman, H. Abdullah, T.S. Kiong, N. Amin, Mater. Res. Express **5**, 096409 (2018)
56. D. Yazıcı, M. Erdem, B. Özçelik, J. Supercond. Novel Magn. **25**, 725–729 (2012)
57. A. Polasek, P. Majewski, E.T. Serra, F. Rizzo, F. Aldinger, Mater. Res. **7**, 393–408 (2004)
58. M.M. Abbas, L.K. Abbas, U. Salman, Energy Procedia **18**, 215–224 (2012)
59. C.P. Bean, Phys. Rev. Lett. **8**, 250–253 (1962)
60. B. Heeb, L.J. Gauckler, J. Mater. Res. **8**, 2170–2176 (1993)